Two-neutron and core-excited states in ^{210}Pb: Tracing $E3$ collectivity and evidence for a new β-decaying isomer in ^{210}Tl

R. Broda,[1] Ł. W. Iskra,[1] R. V. F. Janssens,[2] B. A. Brown,[3] B. Fornal,[1] J. Wrzesiński,[1] N. Cieplicka-Oryńczak,[1] M. P. Carpenter,[4] C. J. Chiara,[4,5,*] C. R. Hoffman,[4] F. G. Kondev,[4] G. J. Lane,[6] T. Lauritsen,[4] Zs. Podolyák,[7] D. Seweryniak,[4] W. B. Walters,[5] and S. Zhu[4]

[1]*Institute of Nuclear Physics, Polish Academy of Sciences, PL-31-342 Kraków, Poland*
[2]*Department of Physics and Astronomy, University of North Carolina at Chapel Hill, Chapel Hill, North Carolina 27599, USA and Triangle Universities Nuclear Laboratory, Duke University, Durham, North Carolina 27708, USA*
[3]*Department of Physics and Astronomy and National Superconducting Cyclotron Laboratory, Michigan State University, East Lansing, Michigan 48824-1321, USA*
[4]*Physics Division, Argonne National Laboratory, Argonne, Illinois 60439, USA*
[5]*Department of Chemistry and Biochemistry, University of Maryland, College Park, Maryland 20742, USA*
[6]*Department of Nuclear Physics, Research School of Physics & Engineering, Australian National University, Canberra, A. C. T. 2601, Australia*
[7]*Department of Physics, University of Surrey, Guildford GU2 7XH, United Kingdom*

(Received 11 May 2018; published 31 August 2018)

Yrast and near-yrast levels up to an $I = 17\hbar$ spin value and a 6-MeV excitation energy have been delineated in the "two-neutron" ^{210}Pb nucleus following deep-inelastic reactions involving ^{208}Pb targets and a number of heavy-ion beams at energies ∼25% above the Coulomb barrier. The level scheme was established on the basis of multifold prompt and delayed coincidence relationships measured with the Gammasphere array. In addition to the previously known states, many new levels were identified. For most of the strongly populated states, spin-parity assignments are proposed on the basis of angular distributions. The reinvestigation of the $\nu(g_{9/2})^2$, 8^+ isomeric decay results in the firm identification of the low-energy $E2$ transitions involved in the $8^+ \rightarrow 6^+ \rightarrow 4^+$ cascade, and in a revised 6^+ level half-life of 92(10) ns, nearly a factor of 2 longer than previously measured. Among the newly identified states figure spin $I = 4$–$10\hbar$ levels associated with the $\nu g_{9/2} i_{11/2}$ multiplet, as well as yrast states involving $\nu g_{9/2} j_{15/2}$, $\nu i_{11/2} j_{15/2}$, and $\nu(j_{15/2})^2$ neutron couplings. The highest-spin excitations are understood as $1p$-$1h$ core excitations and the yrast population is found to be fragmented to the extent that levels of spin higher than $I = 17\hbar$ could not be reached. Four $E3$ transitions are present in the ^{210}Pb yrast decay; three of these involve the $g_{9/2} \rightarrow j_{15/2}$ octupole component, as reflected in the 21(2) and > 10 Weisskopf unit enhancements of the $B(E3)$ rates of the first two. The fourth, $16^+ \rightarrow 13^-$ $E3$ transition corresponds to the 3^- core octupole excitation built on the $\nu i_{11/2} j_{15/2}$ state, in analogy to a similar $E3$ coupling to the $\nu j_{15/2}$ level in ^{209}Pb. Shell-model calculations performed for two-neutron states and $1p$-$1h$ ^{208}Pb core excitations are in good agreement with the data. Evidence was found for the existence of a hitherto unknown high-spin β-decaying isomer in ^{210}Tl. Shell-model calculations of the ^{210}Tl levels suggest the possibility of a 11^+ long-lived, β-decaying state, and the delayed yields observed in various reactions fit rather well with a ^{210}Tl assignment.

DOI: 10.1103/PhysRevC.98.024324

I. INTRODUCTION

Recent investigations of the level structure of "doubly magic" ^{208}Pb have provided important new insight on both the low-spin [1] and high-spin [2] parts of its level scheme. Heussler *et al.* [1] used a combination of (p, p'), (d, d'), and (d, p) reactions to study with high resolution levels with spin I up to $12\hbar$ and excitation energy up to about 6.2 MeV. As a result of the detailed examination of the new data, in combination with all the information available previously, 151 states were firmly established and given unique spin-parity assignments. Furthermore, a good understanding of the intrinsic structure of most of these levels was provided. In parallel with the efforts of Ref. [1], γ-ray spectroscopy studies exploiting the power of deep-inelastic heavy-ion reactions (DIHIRs) [3], resulted in a ^{208}Pb level scheme extended to the highest angular momenta observed thus far: states up to an excitation energy of 16.4 MeV and a spin range of $I \sim 32\hbar$ were reported in Ref. [2]. Most of the high-spin levels, including three new isomeric states, were assigned firm spin-parity quantum numbers. This includes the highest-lying, long-lived 28^- isomer at 13.7 MeV which was proposed to be associated with the first yrast $3p$-$3h$ core excitation in ^{208}Pb. Above this isomer, an additional group of 11 transitions was identified and some of these were placed in a sequence extending up to at least $I = 32\hbar$. It is noteworthy that the observed ^{208}Pb yrast

[*]Present address: US Army Research Laboratory, Adelphi, Maryland 20783, USA.

decay points to a particular role for $E3$ collectivity, as inferred from the presence of strongly enhanced [up to 56 Weisskopf units (W.u.)] $E3$ transitions.

All of these new experimental results concern ^{208}Pb, a nucleus central to a region of the periodic chart thought to play an important role in evaluating the applicability of the shell model for the description of large nuclear systems. Results of large-scale shell-model calculations agree rather well with the ^{208}Pb data for a large number of levels, at least up to an $I = 19\hbar$ spin value [1,2]. However, at higher spins, comparisons between experimental and calculated level energies are less satisfactory [2]. In fact, at this point, theory hardly provides guidance suitable for interpreting the structure of the higher-lying yrast levels, including the isomeric states. Whereas refinements of these rather complex calculations remain a challenging task for theory, it is possible that new experimental information on other nuclei in the ^{208}Pb region will provide additional input to improve present understanding. For example, delineating excitations associated with rather simple configurations in these neighboring systems may shed additional light on the relevant single-particle structure and the relative importance of the interactions involved. With this aim, high-spin levels in ^{210}Pb have been reexamined in the present work using the extensive set of DIHIR data that was exploited in the ^{208}Pb study of Ref. [2].

The results of previous experimental investigations of ^{210}Pb have been reviewed and summarized in Ref. [4]. These were based mostly on a study of ^{210}Tl β decay [5] that, together with data from (t, p) [6] and $(t, p\gamma)$ [7] reactions, established the low-spin part of the level scheme. The high-spin levels were investigated in earlier DIHIR experiments using γ-ray spectroscopy techniques [8,9]. The resulting ^{210}Pb level scheme was fairly well developed, but spin-parity assignments remained speculative in the absence of multipolarity information. As will be demonstrated in the following, the set of much improved DIHIR spectroscopy data available in the present work made it possible to clarify a number of open questions regarding the existing level scheme, also in its low-spin part, and enabled a significant extension of the experimental information on the ^{210}Pb levels.

II. EXPERIMENTAL PROCEDURES AND DATA ANALYSIS

The ^{210}Pb nucleus was produced in the same series of γ-ray spectroscopy experiments on which the ^{208}Pb work of Ref. [2] was based. The measurements were all performed at Argonne National Laboratory. The data set obtained with a 75-mg/cm^2-thick, 99% enriched ^{208}Pb target bombarded by a 1440-MeV ^{208}Pb beam provided coincidence spectra with the highest statistics and the best peak-to-background ratio. As a result, this set was used most in the present study. However, other data from experiments with ^{48}Ca, ^{76}Ge, and ^{82}Se beams bombarding the ^{208}Pb target, as well as with ^{48}Ca and ^{208}Pb beams on ^{238}U targets, all at energies 15–25% above the respective Coulomb barriers, also contributed to the analysis by providing opportunities to cross-check some of the identifications and confirm complex coincidence relationships. All the heavy-ion beams were provided by the ATLAS superconducting linear accelerator and, in every case, a pulsing with a 412-ns repetition rate and an intrinsic pulse width of about 0.3 ns was used in order to enable isomer detection between beam bursts.

Gamma rays were collected in a standard coincidence mode with the Gammasphere array [10]. The spectrometer consisted of 101 Compton-suppressed, high-purity germanium detectors. The trigger enabled the recording of all multifold coincidence events, including the twofold ones that proved essential in investigations of isomer decays. Furthermore, in specific cases, these lower-fold events were also essential to achieve suitable statistical accuracy without giving up selectivity for the γ-ray sequences of interest. This was particularly important for the angular-distribution analysis and, in general, involved the most intense transitions.

The main part of the analysis employed the three- and higher-fold coincidence events which were sorted into cubes with various timing conditions. In the following, the letter p will be used to indicate prompt γ transitions registered within a 30-ns time range with respect to the beam pulse, while the letter d will denote delayed transitions occurring between the beam bursts in *ad hoc* selected ranges that extended up to 800 ns when necessary. More specific details of the coincidence analysis will be discussed below in conjunction with the presentation of selected parts of the ^{210}Pb level scheme, the determination of isomeric half-lives, as well as when the observation of a new β-decaying isomer in ^{210}Tl is presented. A particular emphasis was also placed in this work on spin-parity assignments based on the angular-distribution analysis as will be described in the section devoted to the high-spin part of the ^{210}Pb level scheme.

III. EXPERIMENTAL RESULTS

A. Reinvestigation of the 8^+ isomer decay

The existence of an 8^+ isomer at an excitation energy of about 1275 keV, with a half-life of 201(17) ns, has been well established in previous studies [4], where the state has been associated with the stretched $\nu(g_{9/2})^2$ neutron configuration. Its decay has been delineated and found to proceed via a sequence of levels with the same $\nu(g_{9/2})^2$ character, including the 6^+, 49(6)-ns isomer. However, because of their low energies, the $8^+ \rightarrow 6^+$ and $6^+ \rightarrow 4^+$ transitions had thus far only been determined with large uncertainties that translated into a poor determination of the excitation energies, not only for the two levels involved, but also for all higher-lying states [4]. As listed in Table I, the present data enabled the more precise identification of the 80.2(2)- and 97.6(1)-keV γ rays as the isomeric transitions from the 8^+ and 6^+ long-lived states, respectively, herewith providing the desired more precise energy determinations that remove the 3-keV uncertainty adopted previously. Moreover, the $4^+ \rightarrow 2^+$, 298(1)-keV transition energy has now been determined as 297.4(1) keV, so that the entire sequence of $\nu(g_{9/2})^2$ states is now established with good precision. Representative coincidence spectra are displayed in Fig. 1 in order to highlight the identification of the low-energy transitions under discussion. The upper spectrum in Fig. 1(a) was obtained from the *pdd* cube in the ^{208}Pb + ^{208}Pb data by placing coincidence gates on the

TABLE I. List of levels and depopulating transitions observed in ^{210}Pb. Firm spin-parity assignments and transition multipolarities are based on angular-distribution results; tentative assignments are given in parentheses. Multipolarities of weaker transitions are often inferred from the level scheme, The relative transition intensities, normalized to the 100 units adopted for the 528.1-keV γ-ray intensity, represent the level population observed in the ^{208}Pb + ^{208}Pb reaction.

E_{level} (keV)	I^{π}_{initial}	E_{γ} (keV)	I^{π}_{final}	Multipol.	γ intensity
799.6	2^+	799.6(1)	0^+	$E2$	99.0[a]
1097.0	4^+	297.4(1)	2^+	$E2$	87(4)[a]
1194.6	6^+	97.6(1)	4^+	$E2$	12.7(8)[a]
1274.8	8^+	80.2(2)	6^+	$E2$	5.3(11)[a]
1802.9	10^+	528.1(1)	8^+	$E2$	100.0
1873.0	3^-	1073.4(4)	2^+	$E1$	1.3(4)[b]
1959.0	(4^+)	862.0(5)	4^+	$(M1)$	3.5(5)[b]
2006.5	(8^+)	731.7(2)	8^+	$(M1)$	10.5(4)
2032.8	5^+	838.0(4)	6^+	$M1$	3.4(7)
		935.8(2)	4^+	$M1$	5.2(5)[b]
2043.6	$(6^+, 7^+)$	849.0(5)	6^+	$(M1)$	4.0(5)
2059.0	$(6^+, 7^+)$	864.4(5)	6^+	$(M1)$	5.2(6)
2115.1	9^+	312.3(1)	10^+	$M1$	3.4(3)
		840.2(1)	8^+	$M1$	7.6(5)
2508.4	11^-	393.4(2)	9^+	$M2$	1.5(3)
		705.5(2)	10^+	$E1$	5.9(8)
		1233.6(1)	8^+	$E3$	101.8(25)
2859.9	(10^+)	1057.0(5)	10^+	$(M1)$	1.0(4)
3149.1	13^-	640.7(1)	11^-	$E2$	47.6(12)
		1346.1(1)	10^+	$E3$	28.2(12)
3212.2	12^-	703.8(2)	11^-	$M1$	7.8(9)
3289.7	(11^-)	1486.8(5)	10^+	$(E1)$	1.0(7)
4130.2	14^+	981.0(1)	13^-	$E1$	28.2(6)
		1622.0(2)	11^-	$E3$	3.6(5)
4751.8	14^-	1602.7(1)	13^-	$M1 + E2$	20.9(13)
4794.1	(14^-)	1645.0(3)	13^-	$(M1 + E2)$	3.0(3)
5047.0	(14^+)	916.8(2)	14^+		1.6(3)
		1898.5(6)	13^-		0.6(2)
5150.9		1020.7(4)	14^+		2.8(6)
5185.7	15^-	433.9(2)	14^-	$M1$	3.6(3)
5366.0		215.1(2)			2.1(4)
5417.1	(15^+)	370.1(2)	(14^+)		1.8(3)
		1287.0(2)	14^+	$(M1)$	1.4(3)
5542.4	(15^-)	790.6	14^-	$(M1)$	2.3(2)
5596.7	16^+	410.9(2)	15^-	$E1$	3.2(3)
		1466.6(3)	14^+	$E2$	3.5(3)
		2447.7(3)	13^-	$E3$	3.9(3)
5600.6		1470.4(3)	14^+		2.4(2)
5686.9	$15^{(-)}$	270.1(3)	(15^+)	$(E1)$	1.5(3)
		1556.7(1)	14^+	$(E1)$	5.7(4)
5800.2	(16^+)	1670.0(5)	14^+	$(E2)$	1.0(4)
5836.9	17^+	240.2(1)	16^+	$M1$	3.6(3)

[a]Relative γ-ray intensities calculated using experimentally determined electron conversion coefficients and normalized to the 100 units of the 8^+ isomer decay.

[b]Transitions identified and located in ^{210}Pb on the basis of prompt coincidence relationships with the 800- and/or 297-keV γ rays as well as with transitions from the complementary reaction partner ^{206}Pb.

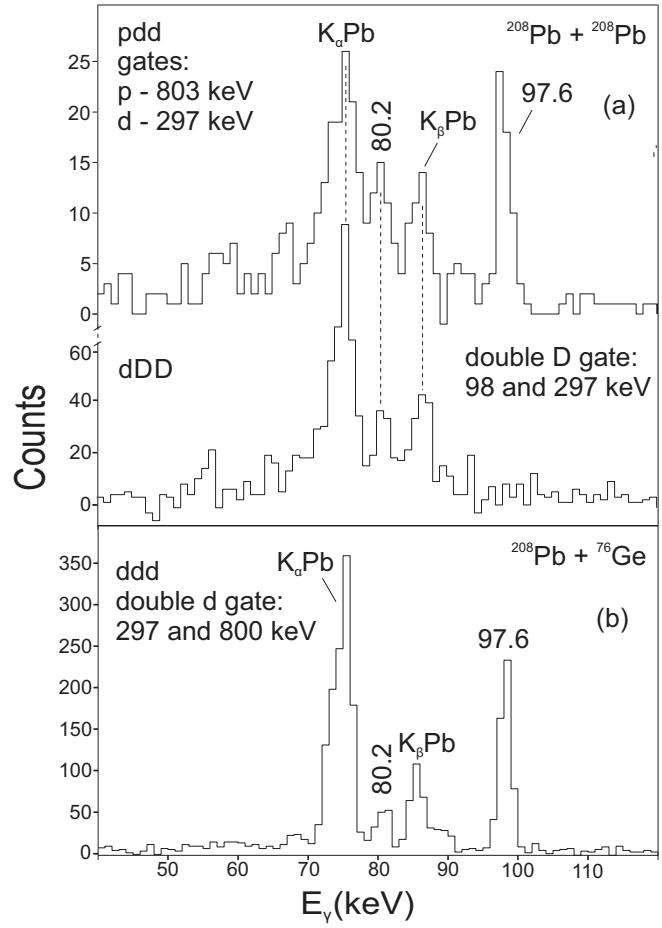

FIG. 1. Examples of low-energy γ-ray spectra used to identify the 80.2-keV, $8^+ \rightarrow 6^+$ and 97.6-keV, $6^+ \rightarrow 4^+$ transitions in the ^{210}Pb, 8^+ isomer decay. (a) Spectra from the ^{208}Pb + ^{208}Pb reaction data where the upper one is from the *pdd* coincidence cube with a double coincidence gate placed on the prompt (p) 803-keV transition in the ^{206}Pb reaction partner and the delayed (d) 297-keV line in ^{210}Pb. The lower spectrum in (a) is from the dDD cube with a double gate placed on the axes with longer delay (D) for the 98- and 297-keV γ rays, in order to demonstrate that the less-delayed (d) 80.2-keV transition precedes in time the 6^+ isomer (see text). (b) Coincidence spectrum from the ^{76}Ge + ^{208}Pb data in the delayed ddd coincidence cube, where a double gate was placed on the 297- and 800-keV ^{210}Pb transitions along the two axes where a broad-range delayed time condition was required (see text).

prompt (p) 803-keV transition in the ^{206}Pb reaction partner and delayed (d) 297-keV line in ^{210}Pb. Apart from the intense 97.6-keV, $6^+ \rightarrow 4^+$ transition, the weaker 80.2-keV γ ray is clearly visible and is identified as the strongly converted $8^+ \rightarrow 6^+$ $E2$ transition. The lower spectrum in Fig. 1(a) was extracted from the dDD cube with gates set on the 98- and 297-keV transitions with the long time delay (D) to demonstrate that the less-retarded (d) 80.2-keV line precedes in time the deexcitation from the 6^+ level that also exhibits a long half-life. In ^{208}Pb + ^{208}Pb collisions, Pb x rays are

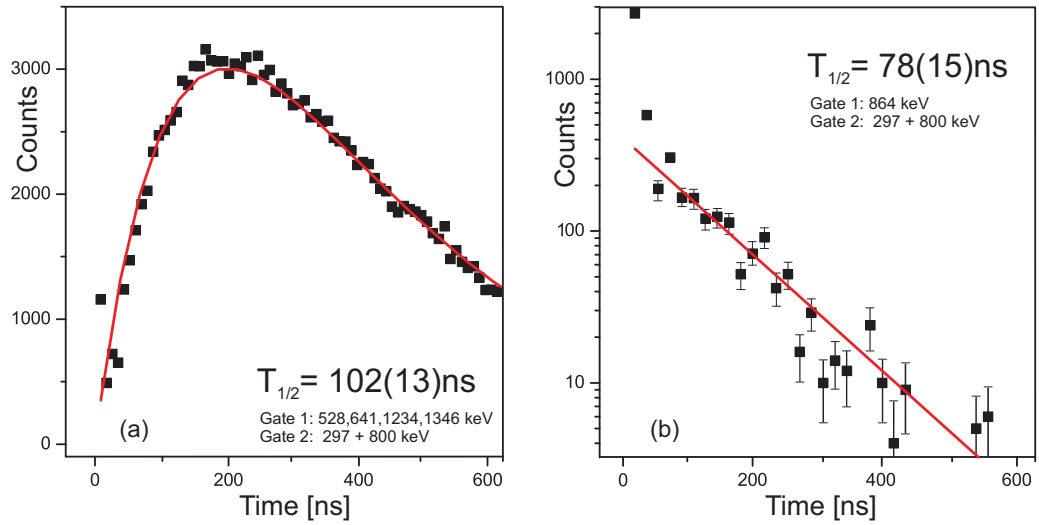

FIG. 2. Time distributions used to determine the half-life of the 6^+ state in ^{210}Pb. (a) Time distribution between the prompt γ rays populating the 8^+ isomer (see legend: Gate 1) and delayed transitions depopulating the 4^+ state (Gate 2). The fit shown by the red line assumes a sequential decay where the previously measured 201(17) ns half-life of the 8^+ isomer [7] is adopted and the half-life of the 6^+ state is found to be $T_{1/2} = 102(13)$ ns. (b) Time distribution obtained with the same delayed coincidence gates (Gate 2) as in (a), but with a prompt gate placed on the 864-keV transition that populates the 6^+ level directly (Gate 1). The resulting fit of the decay curve corresponds to $T_{1/2} = 78(15)$ ns half-life, consistent within errors with the value in panel (a) and, as a result, an average value of $T_{1/2} = 92(10)$ ns was adopted for the 6^+ state half-life (see text).

abundantly produced with energies broadened by Doppler effects. This impacts the quality of low-energy spectra, and therefore Fig. 1(b) provides the delayed coincidence spectrum obtained from the ^{76}Ge + ^{208}Pb data with 297- and 800-keV gates placed in the *ddd* coincidence cube in order to confirm the presence of the 80.2-keV transition. It should be noted that the intensity balance observed for transitions involved in the 8^+ isomer decay allowed for the determination of total internal electron conversion coefficients (ICCs), herewith confirming their $E2$ character. The measured ICC values of 0.15(4), 6.9(5), and 18(4) agree well with theoretical ones of 0.12, 7.0, and 16.4 calculated for the 297.4-, 97.6-, and 80.2-keV $E2$ transitions, respectively.

Respective half-life values of 201(17) and 49(6) ns were determined for the 8^+ and 6^+ levels in studies devoted mainly to g-factor measurements where these states were populated with the $(t, p\gamma)$ reaction [7]. The present data are consistent with the 201-ns, 8^+ state half-life and this value is adopted as it was measured with a long, 1.7-μs time range [7] more suitable for such a determination than the one available in this work when considering that equilibrium should be reached in a sequential decay involving two long-lived levels. On the other hand, the present data required a revision of the 6^+ state half-life. The time distribution displayed in Fig. 2(a) was obtained by placing the energy gates on transitions feeding the 8^+ isomer together with the 297- and 800-keV γ rays located below the 6^+ long-lived state. The growth with time of the 6^+ isomeric yield in this sequential decay is significantly slower than would be expected for the 49-ns half-life. In fact, fits of the sequential decay curve in which the 8^+ state half-life was fixed at the two extremes defined by the 201(17)-ns accuracy resulted in an average value of 102(13) ns for the half-life of the 6^+ state. In the subsequent analysis discussed below, three new transitions populating the 6^+ state were identified. Of those, the 864-keV γ ray was found to be most suitable for an additional determination of the 6^+ half-life and the corresponding time distribution is presented in Fig. 2(b). The 78(15)-ns value overlaps with the result of Fig. 2(a) and a 92(10)-ns weighted average is adopted here as the half-life, a value larger by nearly a factor of 2 than that determined in Ref. [7]. It should be noted that, while the high statistical precision of the data presented in Ref. [7] allowed a precise half-life determination for the 8^+ state, the extraction of a value for the 6^+ level was less straightforward, as it required a rather complex fitting of a sequential decay together with a component due to the direct population of the 6^+ level. The latter contribution was included as an additional free parameter into the fit and was determined to be 35% of the 6^+ level population in the (t, p) reaction. Variations in the magnitude of this contribution would affect the half-life value. The present determination relies on coincidence data which do not suffer from a similar direct feeding issue, since only events associated with the population of the 6^+ level in the 8^+ isomeric decay are selected.

B. Identification of $\nu g_{9/2} i_{11/2}$ states

The ^{210}Pb level scheme established in the present study is displayed in Fig. 3, and Table I provides the list of energies and intensities measured for all observed levels and γ-ray transitions. Among high-spin states, which will be discussed in the next subsection, figures the strongly populated yrast 10^+ level at 1802.9 keV that can be identified as the highest-spin state arising from the coupling of $g_{9/2}$ and $i_{11/2}$ neutrons. Here, the analysis dedicated to the search for other members of this $\nu g_{9/2} i_{11/2}$ multiplet is described first, as these states are

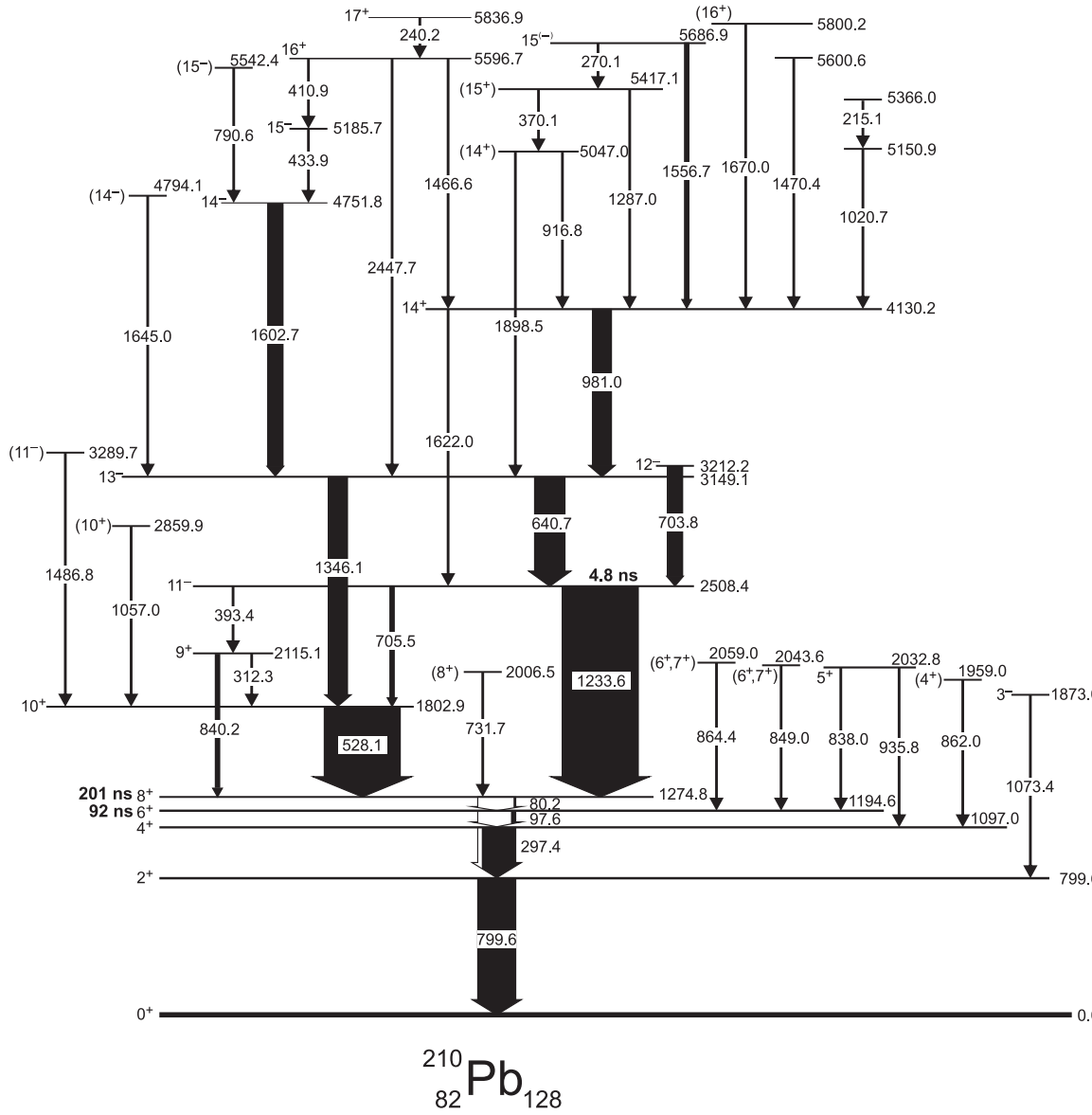

FIG. 3. The ^{210}Pb level scheme established in the present work. The widths of the arrows reflect the intensities involved in the prompt population of the various states, except for transitions below the 8^+ isomer, where an arbitrary width represents the total isomer decay intensities including the electron conversion portion, in white. See text for details on the construction of the level scheme and on the spin-parity assignments.

expected to fall well within the excitation energy–spin window populated in the $2n$-transfer reaction used in the present study. Moreover, the $M1$ transitions connecting these states with the corresponding $\nu(g_{9/2})^2$ levels should be observed as discrete lines free of the Doppler broadening, since they are expected to be associated with state half-lives of the same order of magnitude as the 8.2-ps l forbidden $i_{11/2} \rightarrow g_{9/2}$ $M1$, 778.8-keV transition in ^{209}Pb [11]. In the analysis, the data from all experiments listed in Sec. II were used to cross-check the identification of transitions first made on the basis of the ^{208}Pb + ^{208}Pb experiment. Relevant coincidence spectra from the latter measurement are presented in Fig. 4. All these spectra were obtained by placing double gates on the 297- and 800-keV transitions in threefold coincidence cubes sorted with appropriate timing conditions. The spectrum of Fig. 4(a) is from the prompt ppp cube (0–30-ns range) and exhibits the 862- and 936-keV γ rays that feed the 4^+ yrast level directly. It may be noted that, apart from transitions located above the 8^+ isomer in ^{210}Pb, such as the 528- and 981-keV lines for example, the spectrum shows predominantly transitions from the ^{206}Pb reaction partner. The relative intensities of these γ rays reflect the population of low-spin ^{206}Pb states accompanying the prompt population of the 4^+ level in ^{210}Pb and is characteristic of a peripheral, quasielastic $2n$-transfer reaction. In order to enhance the observation of prompt transitions populating the 6^+ isomer, the spectrum displayed in Fig. 4(b) was obtained from the pdd coincidence cube, where the gating 297- and 800-keV transitions were required to be observed within the 20–70-ns delayed time range. This coincidence spectrum allowed for the identification of three

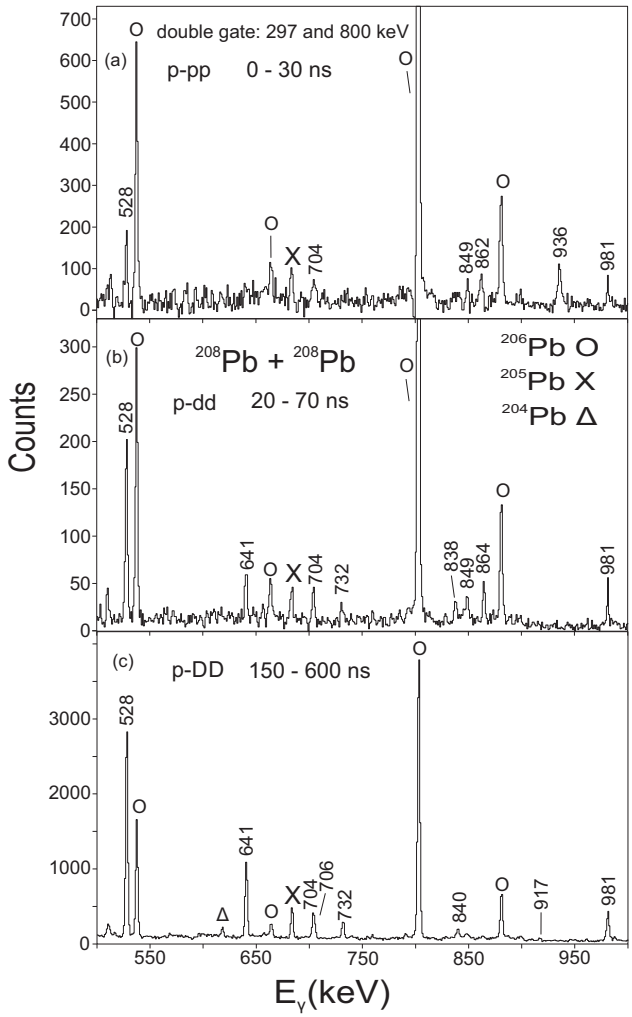

FIG. 4. Examples of coincidence spectra instrumental in identifying the $\nu g_{9/2} i_{11/2}$ states in ^{210}Pb. In all of these, prompt γ rays are displayed that are found to be in coincidence, within selected time ranges, with double gates placed on the 297- and 800-keV γ rays located below the 4^+ level in ^{210}Pb. Transitions arising from reaction-partner Pb isotopes are marked by the various symbols given in the legend. (a) Spectrum obtained with a prompt double gate showing the 862- and 936-keV transitions populating the 4^+ level. (b) The short delay placed on the gating transitions enabled the identification of the 838-, 849-, and 864-keV γ rays populating the 6^+ isomer. (c) Requiring the longest delay for the gating transitions allows one to distinguish the 528-, 732-, and 840-keV lines as populating the 8^+ isomer (see text for further details).

new transitions of 838, 849, and 864 keV that populate the 6^+ level directly. Finally, the pDD cube, with the long delay range of 150–600 ns, was used to obtain the spectrum of Fig. 4(c), where γ rays located above the 8^+ isomer can be observed. Among the strong yrast transitions that will be discussed below, one can distinguish the 732- and 840-keV γ rays that feed the 8^+ state directly and correspond to the anticipated $M1$ transitions from the $\nu g_{9/2} i_{11/2}$ levels.

Results of this search for the $\nu g_{9/2} i_{11/2}$ states can be summarized by assigning spin values to the newly observed states, based primarily on the expectation that this sequence of levels should extend across the $I = 1$–10 spin range. Although, as will be discussed later, spin and parity could be rigorously assigned only for the 1803-keV 10^+ state, the assignments to other levels, which are based mostly on the observed depopulation pattern, are considered to be rather firm in view of the simple level structure expected in the ^{210}Pb isotope within this range of excitation energies. These assignments can be found in the scheme of Fig. 3 and are supported by the following arguments. Only two levels at 2115.1 and 2006.5 keV, depopulated by transitions feeding the 8^+ isomer, can be considered as candidates for the expected 8^+ and 9^+ states of the multiplet. Of those, the 9^+ spin parity is assigned to the 2115.1-keV level as it is depopulated by the 312-keV transition to the 10^+ state in competition with the 840-keV branch to the 8^+ isomer. Both of these competing transitions are most likely of $M1$ character and the comparison of the $B(M1)$ reduced probabilities indicates that the 312-keV one is faster by a factor 9, as should be expected for a $M1$ transition between $\nu g_{9/2} i_{11/2}$ states when compared to the retarded $M1$ decay to the $\nu(g_{9/2})^2$ level. In addition, the 2115.1-keV state is populated by the 393-keV γ ray, associated with the $M2$ decay from the firmly established 11^- state (see below), thereby confirming the 9^+ assignment. Consequently, the 2006.5-keV level is assigned as the 8^+ state and, in the absence of measurable feeding from higher-lying levels, the relatively strong 732-keV transition to the 8^+ isomer indicates its direct population with a yield consistent with expectation for such a 8^+_2 state. The 2059.0- and 2043.6-keV levels were established through the observation of the 864- and 849-keV γ rays depopulating them to the 6^+ state, respectively. This depopulation pattern defines both of these as good candidates for respective 6^+ and 7^+ assignments. However, since both are populated with a similar yield and since a search for an $M1$ decay to the 8^+ isomer was unsuccessful in both cases, the issue of which spin-parity assignment should be given to which level remains unresolved and $(6^+, 7^+)$ assignments are proposed for both states in Fig. 3. In contrast, the 2032.8-keV level can be uniquely assigned as the 5^+ state, based on the observed depopulation by 838- and 936-keV $M1$ transitions characterized by close $B(M1)$ rates to the 6^+ and 4^+ levels, respectively. The 1959.0-keV level depopulated by the 862-keV γ ray to the 4^+ level can then be tentatively assigned as the 4^+ level, herewith representing the lowest-spin $\nu g_{9/2} i_{11/2}$ state observed in the present work. The remaining 3^+, 2^+, and 1^+ levels of this multiplet could not be established as their expected decay pattern does not offer any means for selective identification in the present study.

It should be noted that the 1.95(3)- and 2.00(3)-MeV levels observed in the β decay of the ^{210}Tl (5^+) ground state with the energy resolution of scintillator detectors [5] are likely identical to the (4^+), 1959.0-keV and (5^+), 2032.8-keV states observed in the present work and the spin-parity assignments proposed earlier agree with those adopted here. Similarly, several levels observed with 15-keV energy resolution in the (t, p) reaction of Ref. [6] can likely be associated with levels observed here. However, for most of these, a firm correspondence could not be established since the transitions remained unassigned in Ref. [6]. On the other hand, the 1870(10)-keV state, uniquely identified in several earlier studies as being the

3^- level [4], was also observed here. The weak, 1073.4-keV γ ray feeding the 799.6-keV, 2^+ state in ^{210}Pb was clearly seen in the data from all the experiments described in Sec. II when the coincidence selectivity was enhanced by requiring the detection of the 800-keV, $2^+ \rightarrow 0^+$ line in ^{210}Pb together with transitions in corresponding partner nuclei in the $2n$-transfer reaction. A more precise energy of 1873.0(4) keV has now been obtained for this 3^- level (Fig. 3 and Table I).

C. High-spin states above the 8^+ isomer

The half-life of the 8^+ isomer provided the selectivity required to identify and delineate higher-lying sequences of transitions by means of delayed-coincidence techniques. The spectrum of prompt γ rays preceding in time the isomeric decay is displayed in Figs. 5(a) and 5(b). It was obtained from the ^{208}Pb + ^{208}Pb data using the *pdd* coincidence cube with double gates placed on the delayed (d) 297- and 800-keV transitions. Most of the ^{210}Pb transitions are indicated by their energies and those arising from reaction partners, predominantly ^{206}Pb, are marked with the symbols given in the legend. This high-spin part of the scheme was delineated mostly with the help of a prompt coincidence *pp* matrix selected from the *ppd* cube with single gates on the 297- and 800-keV delayed (d) transitions. The present coincidence analysis confirmed the main part of the level scheme first reported in Ref. [8], and discussed more completely in Ref. [9]. Therefore, only the few modifications to the earlier work resulting from this analysis will be discussed here, and the main emphasis is placed below on spin-parity assignments, the main contribution from the present investigation.

As discussed in Ref. [2], the angular-distribution results obtained in the ^{208}Pb study were facilitated by the large degree of spin alignment observed in the ^{208}Pb + ^{208}Pb reaction. The same feature of significant spin alignment holds in the ^{210}Pb case. The angular-distribution analysis allowed for the unique characterization of the most important transitions and provided firm spin-parity assignments to many of the high-spin levels above the 8^+ isomer. For most γ rays, the angular-distribution data and the accompanying fits are displayed in Fig. 6, and the numerical results obtained for the A_2 and A_4 coefficients are listed in Table II. Note that for six weaker transitions the A_4 term was neglected in the fitting procedure.

Among the four most intense transitions above the 8^+ isomer, the angular distributions characterize the 528.1- and 640.7-keV pair as being of stretched-$E2$ character and the higher-energy 1233.6- and 1346.1-keV γ rays as stretched-$E3$ ones. These observations settle the spin-parity assignments of $I^\pi = 10^+, 11^-$, and 13^- to the 1802.9-, 2508.4-, and 3149.1-keV states, respectively. These results also confirm the earlier tentative assignments of Refs. [8,9], which were merely based on shell-model expectations. The 12^- spin parity assigned to the 3212.2-keV level follows from the anisotropy of the 703.8-keV γ ray, which is compatible with a $\Delta I = 1$, $M1$ transition. This assignment is also supported by the absence of any detectable feeding of this level from higher-lying states, as is to be expected for levels located away from the main yrast decay sequence. This part of the level scheme (Fig. 3) also includes the newly placed 393.4-keV transition discussed

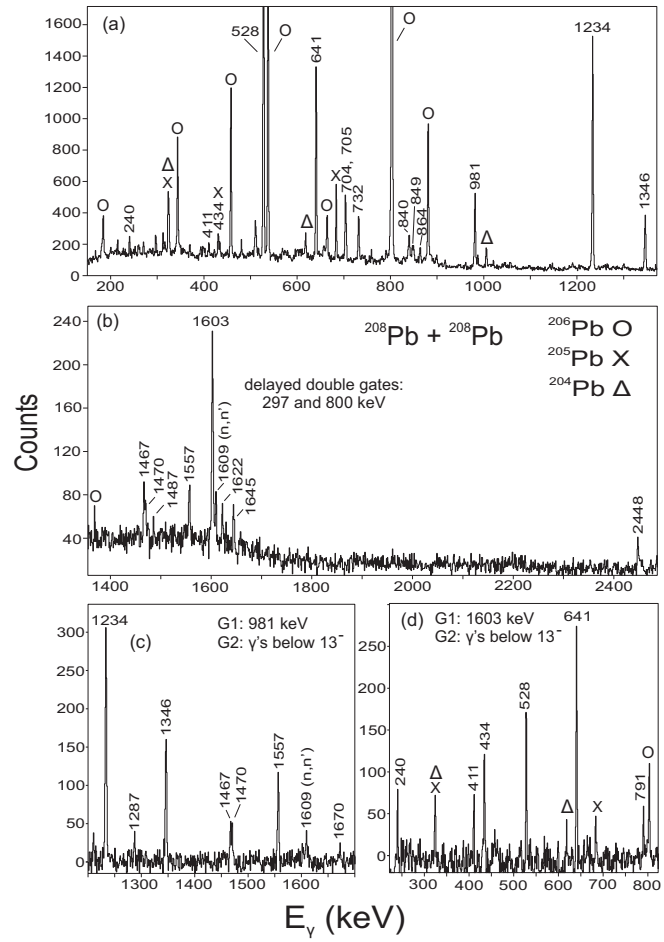

FIG. 5. Examples of coincidence spectra addressing the part of the ^{210}Pb level scheme located above the 8^+ isomer. (a),(b) Low- and high-energy parts of the prompt spectrum displaying γ rays preceding in time the isomeric decay obtained by placing a double gate on the 297- and 800-keV delayed transitions. The ^{208}Pb + ^{208}Pb data were used, therefore γ lines arising from reaction-partner Pb isotopes are present, and identified by the symbols given in the legend. (c) Partial spectrum from the prompt *ppp* cube with double gates on the 981-keV transition and on the four most intense γ rays below the 13^- level. The energy range of this spectrum is such that the main transitions populating the yrast 14^+ state are visible. (d) Spectrum obtained in the same way, but with the first gate placed on the 1603-keV transition so that all the transitions observed above the yrast, 4752-keV, 14^- level are visible (see Fig. 3 and text).

in Sec. III B and the two new γ rays of 1057.0 and 1486.8 keV feeding the yrast 10^+ state from the 2859.9- and 3289.7-keV levels, respectively. Although both states are weakly populated, their identification is firm and both have likely been observed with poorer energy resolution in the earlier (t, p) reaction [4,6]. Only tentative spin-parity assignments are proposed for these levels in Fig. 3 in view of their weak population.

As discussed below, the confirmation of the $I^\pi = 14^+$ assignment to the 4130.2-keV level is important and validates the earlier, tentative one of Refs. [8,9] suggested solely on the basis of shell-model considerations. The relatively

TABLE II. Angular-distribution results for transitions in ^{210}Pb above the 8^+, 1275-keV isomer. The columns include the transition and initial level energies, the spin-parity assignments for the initial and final states, the numerical values of the fitted A_2 and A_4 angular-distribution coefficients, and the adopted transition multipolarity, respectively. The absence of an A_4 value indicates an instance where the fit included only the A_2 term. The $\alpha_2 = 0.65$ coefficient adopted for ^{208}Pb in Ref. [2] to describe the reduction in the A_2 angular distribution coefficients due to incomplete spin alignment, is apparently also valid for the ^{210}Pb reaction products. This can be concluded from A_2 coefficients obtained for several transitions with a pure multipolarity. For mixed transitions, the quantitative results describing the mixing are not given due to the rather low precision of the measured A_2 coefficients.

E_{gamma}	E_i	I^π_{init}	I^π_{final}	A_2	A_4	multipolarity
528.1	1802.9	10^+	8^+	0.31(6)	−0.09(7)	$E2$
640.7	3149.1	13^-	11^-	0.26(3)	−0.11(4)	$E2$
703.8	3212.2	12^-	11^-	−0.17(7)		$M1$
981.0	4130.2	14^+	13^-	−0.10(8)		$E1$
1233.6	2508.4	11^-	8^+	0.43(4)	−0.14(12)	$E3$
1346.1	3149.1	13^-	10^+	0.40(10)	−0.11(13)	$E3$
1556.7	5686.9	15^-	14^+	−0.26(8)		$(E1)$
1602.7	4751.8	14^-	13^-	−0.64(7)	0.14(8)	$M1 + E2$
1622.0	4130.2	14^+	11^-	0.70(16)		$E3$
1645.0	4794.1	$(15^-, 14^-)$	13^-	0.38(20)		$(E2,\ M1 + E2)$
2447.7	5596.7	16^+	13^-	0.47(27)		$E3$

intense 981.0-keV line exhibits an angular distribution that barely matches expectations for a $\Delta I = 1$, $E1$ transition and, therefore, is not conclusive. However, the new 1622.0-keV crossover transition to the 11^-, 2508.4-keV state was firmly established on the basis of coincidence relationships. Considering the possible scenarios for this transition together with the observed angular distribution leads to a stretched-$E3$ assignment that settles the 14^+ spin-parity assignment to the 4130.2-keV level. It should be noted that the $E3$ branch competing with the 981.0-keV $E1$ one indicates a strong $E1$ retardation. Hence, the possibility of an $M2$ admixture affecting the angular distribution of the 981-keV line cannot be excluded when considering its measured A_2 coefficient.

The upper part of the ^{210}Pb level scheme of Fig. 3 includes many weak transitions and only a limited number of these had been observed previously [9]. Among the latter figures the 240.2-, 410.9-, 433.9-, and 1602.7-keV sequence of transitions linking the highest state observed here with the 13^- level at 3149.1 keV. Note that the measured intensities resulted in a changed ordering for the 410.9- and 433.9-keV γ rays with respect to Refs. [8,9]. The observed large negative A_2 coefficient for the 1602.7-keV line uniquely assigns it a mixed $M1/E2$ character and settles the $I^\pi = 14^-$ assignment to the 4751.8-keV state. As the spin-parity values in this sequence are determined well by the available angular distributions, it must be concluded that the high-energy 2447.7-keV crossover transition depopulating the 5596.7-keV level is of $E3$ character. This is also consistent with the angular distribution (Table II) and fixes the quantum numbers of the 5596.7-keV level as $I^\pi = 16^+$. Note that this γ ray is one of three competing deexcitation branches and appears to mirror a similar transition in ^{209}Pb as will be discussed later. The $I^\pi = 15^-$ assignment to the intermediate level at 5185.7 keV takes into account the fact that the 410.9- and 433.9-keV lines must be of dipole character and that one of these must be an $E1$ transition in order to accommodate the parity change in the sequence. Here, the choice of the 410.9-keV γ ray as being of $E1$ multipolarity is guided by the observed competition between the $E1$ (410.9 keV), $E2$ (1466.6 keV), and $E3$ (2447.7 keV) decay branches depopulating the 5596.7-keV level, as it would otherwise be dominated by a 410.9-keV $M1$ transition. The 240.2-keV γ ray is apparently a $\Delta I = 1$, $M1$ transition depopulating the highest energy $I^\pi = 17^+$ yrast level at 5836.9 keV. This assignment appears to remain without an alternative when considering the absence of any other decay to lower-lying levels and noticing how well the total intensity of the 240.2-keV $M1$ transition matches the population pattern expected for yrast states in DIHIR reactions.

For the other ^{210}Pb levels of Fig. 3, tentative spin-parity assignments are suggested based on the observed population intensities and γ-decay branchings. Only for the relatively intense 1556.7-keV line is the angular distribution pointing to a $\Delta I = 1, l = 1$ transition, in line with the $I = 15$ assignment to the 5686.9-keV level. For the 1645.0-keV γ ray, the angular distribution is less conclusive and, hence, was not taken into consideration. It should also be noted that, in the present analysis, no evidence was found for the existence of the 803- and 1609-keV transitions in ^{210}Pb that were included in the high-spin part of the level scheme in Ref. [9].

The results described above establish the ^{210}Pb level scheme up to nearly 6 MeV excitation and in the $I = 17$ spin range, i.e., much lower than the 16.4 MeV and $I \sim 32$ limits reached in ^{208}Pb [2], and the $I \sim 30$ spin range established in spectroscopy studies with DIHIR of other nuclei in the region such as ^{204}Tl [12] and ^{206}Bi [13]. Since the ^{210}Pb production yields in the reactions under investigation in the present work were sufficient to provide high- statistics data, the inability to extend the level scheme to higher excitation energy and angular momentum is rather unusual. A natural explanation for this observation may reside in the absence of any sequence of levels above $I = 14$ with a distinct yrast character, readily distinguishable by having excitation energies significantly lower than those of other states. As a result, the decay from higher spin levels would be strongly fragmented and populate many near-yrast states with intensities often close to or below

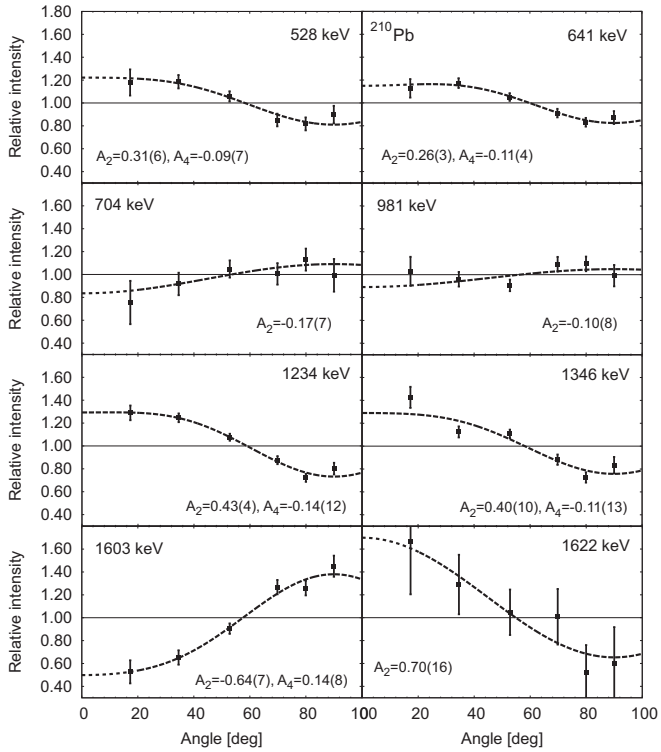

FIG. 6. Sample angular distributions obtained for ^{210}Pb transitions from the ^{208}Pb + ^{208}Pb data set. As described in the text, the data were fitted with the conventional polynomials of order 2 and 4 (i.e., A_2 and A_4 terms) and, exceptionally, with only an A_2 term. Numerical results, including those for three additional transitions, are listed in Table II. The $E3$ transitions (1234, 1346, and 1622 keV) can be distinguished by significantly larger A_2 values than those characteristic of $E2$ transitions (528 and 641 keV). The large negative A_2 value measured for the 1603-keV γ ray assigns it uniquely as a $\Delta I = 1$, mixed $M1/E2$ transition.

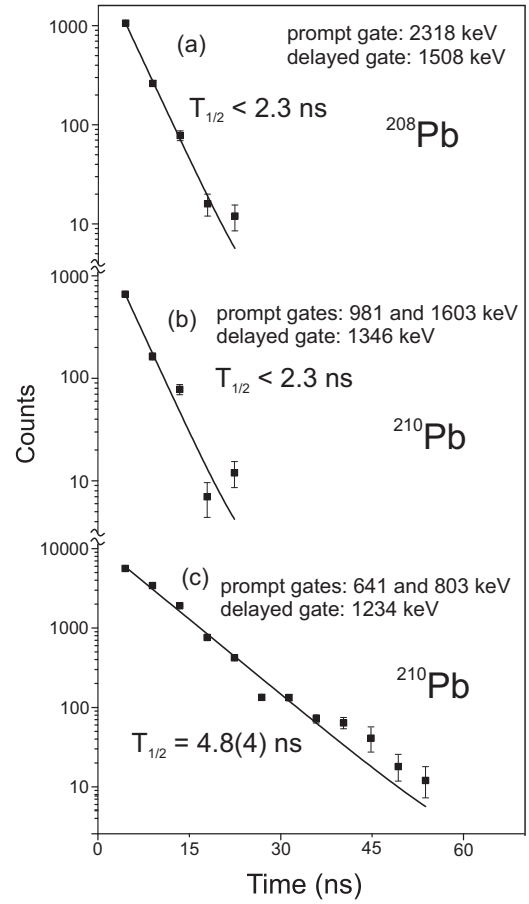

FIG. 7. Time distributions used to determine the half-life of the 11^- level and the half-life limit of the 13^- state in ^{210}Pb. These spectra were obtained by placing gates on the most intense γ rays populating each state from above and on the strongest depopulating transitions as indicated in the figure. (a) Prompt time distribution measured for the strongly populated, short-lived 14^- level in ^{208}Pb [2]. (b) Similar prompt distribution that sets an upper half-life limit for the 13^- level in ^{210}Pb. (c) Half-life determination of $T_{1/2} = 4.8(4)$ ns for the 11^- level in ^{210}Pb. The intense 803-keV transition from the ^{206}Pb reaction partner arises from direct and/or indirect prompt population of the short-lived 2^+ level. It is in prompt coincidence with ^{210}Pb transitions located above the 8^+ isomer and is free of any contribution from higher-lying isomers. It was included in the prompt gate to enhance statistics.

the detection limit. In addition, in the thick target experiments used here, γ rays emitted in flight cannot be observed because of Doppler broadening. Levels with short half-lives (<1 ps) would remain undetected as the associated γ rays would contribute only to the background as a continuum. Below 1700 keV in the spectrum of Fig. 5(b), a rather unusual rise of the continuum beneath the peaks can be noticed, which may possibly arise from such a contribution.

Above the 8^+ isomer, essentially all ^{210}Pb transitions were found within the prompt time window, pointing to the absence of higher-lying isomer(s). A dedicated analysis was devoted to a search for possible short half-lives for the 11^-, 2508.4-keV and 13^-, 3149.1-keV states, since both are depopulated by relatively low-energy $E3$ transitions that could potentially be characterized by half-lives in the nanosecond range despite their anticipated enhancement. The measured time distributions are displayed in Fig. 7, together with the gating transitions associated with the feeding and depopulation of each of these two levels. In Fig. 7(a), the result obtained for the 14^- state in ^{208}Pb, which was estimated to have a 0.4-ns half-life in Ref. [2], is used as an illustration of a prompt time distribution that establishes the 2.3-ns slope as the limiting value for any half-life determination. The nearly identical time distribution of Fig. 7(b) provides a similar upper limit for the 13^-, 3149.1-keV level. For the 11^-, 2508.4-keV level, however, the time distribution in Fig. 7(c) clearly displays a measurable half-life with a value of 4.8(4) ns.

IV. SHELL-MODEL CALCULATIONS AND INTERPRETATION OF ^{210}Pb LEVELS

Shell-model calculations were carried out with the OXBASH code [14]. The model space included all 24 orbitals comprising the four major shells surrounding ^{208}Pb as used in Ref. [15], i.e., proton holes in $(1g_{7/2},\ 2d_{5/2},\ 2d_{3/2},\ 3s_{1/2},\ 1h_{11/2})$ $[\pi\ h]$, proton par-

ticles in $(1h_{9/2},\ 2f_{7/2},\ 2f_{5/2},\ 3p_{3/2},\ 3p_{1/2},\ 1i_{13/2})$ $[\pi\ p]$, neutron holes in $(1h_{9/2},\ 2f_{7/2},\ 2f_{5/2},\ 3p_{3/2},\ 3p_{1/2},\ 1i_{13/2})$ $[\nu\ h]$, and neutron-particles in $(1i_{11/2},\ 2g_{9/2},\ 2g_{7/2},\ 3d_{5/2},\ 3d_{3/2},\ 4s_{1/2},\ 1j_{15/2})$ $[\nu\ p]$ states. The configurations for calculations of ^{210}Pb were truncated to allow for two-neutron particles relative to a closed-shell configuration for ^{208}Pb $[2\nu\ p]$, and two-neutron particles coupled to one-particle one-hole states of ^{208}Pb $[2\nu\ p \times (1p\text{-}1h)]$. The configurations for ^{210}Tl, which will be discussed in the next section, were truncated to allow for three neutron particles coupled to one proton hole $[3\nu\ p \times 1\pi\ h]$.

The Hamiltonian consisted of 24 single-particle energies relative to a closed shell for ^{208}Pb as found in Fig. 1 of Ref. [16]. The two-body matrix elements (TBMEs) for the $[2\nu\ p]$ configurations are those of the modified Kuo-Herling Hamiltonian [17] derived in Ref. [16], where the strength of the particle-hole bubble-diagram contribution to the second-order correction part of the Kuo-Herling interaction between two-neutron particle states was multiplied by a factor of 1.07 in order to improve the agreement with experiment for the calculated energy spectra of ^{211}Pb and ^{212}Pb. The TBMEs required for the $[\nu\ p \times \pi\ h]$ configurations were obtained from Yukawa and one-boson exchange-potential forms with strengths fitted to the relative-coordinate G matrix elements from Ref. [18]. All other TBMEs needed for the particle-hole states were obtained from Yukawa exchange-potential forms with strengths fitted to G matrix elements from [19] (the $M3Y$ potential). These TBMEs were calculated with harmonic-oscillator radial wave functions. No mixing was allowed between the $[2\nu]$ and $[2\nu \times (1p\text{-}1h)]$ configurations of ^{210}Pb. The reason for this approach is that mixing can be carried out only if the $[2\nu]$ part of the Hamiltonian is modified to take into account the fact that $(1p\text{-}1h)$ configurations are explicitly included in the model space (as opposed to their implicit inclusion in the second-order perturbation corrections to the Kuo-Herling matrix elements). This modification is beyond the scope of the present paper. An interpretation of the $E3$ transition strengths that arise from the mixing between the $[2\nu]$ and $[2\nu \times (1p\text{-}1h)]$ configurations cannot be made. Nevertheless, the energy spectra obtained with the unmixed configurations provide guidance for the interpretation of the present experimental results.

The calculated and experimental levels are compared in Fig. 8, where a format similar to that adopted for the experimental level scheme of Fig. 3 is used for clarity. The energies and spin-parity values are indicated for all experimental levels as well as for their theoretical counterparts. In Fig. 8, the computed states are displaced to the right (and drawn in red online).

In the excitation range up to the 14^+, 4130-keV state, the structure is particularly transparent and involves rather pure two-neutron configurations. Here, the observed one-to one correspondence and the satisfactory matching between the calculated and experimental level energies reflect the simple shell-model description of the states involved. Specifically, the 2^+, 4^+, 6^+, and 8^+ levels represent the sequence of nearly pure $\nu(g_{9/2})^2$ states with calculated wave function amplitudes of 94.4, 97.7, 98.6, and 98.9%, respectively. In comparison with Ref. [7], the more precise energy of the $8^+ \rightarrow 6^+$, $E2$ transition established in the present work results in an only slightly larger value of the reduced transition probability $B(E2) = 49(5)\,e^2\,\mathrm{fm}^4$ which corresponds to 0.67(7) W.u. This small change does not alter the discussion presented in Ref. [7] about the $g_{9/2}$ neutron effective charge and the value of $0.88(5)e$ remains valid. However, the much longer half-life of the 6^+ level in the present study, compared to the earlier result [7], yields a strength for the $6^+ \rightarrow 4^+$ transition of $B(E2) = 87(10)e^2\,\mathrm{fm}^4$ that is lower by nearly a factor of 2 and corresponds to 1.19(13) W.u.

The 1873-keV, 3^- state is very weakly populated in the present study and is calculated nearly 400 keV higher in excitation energy than seen experimentally. This is not surprising as this level is understood as a strongly collective state involving a 3^- core excitation enhanced by the involvement of the $g_{9/2} \rightarrow j_{15/2}$ neutron amplitude. A dedicated $(t, p\gamma)$ experiment that would measure the state lifetime and observe the $E3$ γ-decay branch to the ground state would be desirable to clarify the expected increase in the octupole collectivity of this state.

The multiplet of ten states arising from the $g_{9/2}$ and $i_{11/2}$ neutrons coupled to $I^\pi = 1^+\text{–}10^+$ is calculated to be located around 2-MeV excitation energy and to be associated with particularly pure configurations involving $\nu g_{9/2} i_{11/2}$ wave-function amplitudes larger than 99%, with the exception of the calculated 2^+ level (not shown) for which the corresponding value is 96%. The seven highest-spin states of this multiplet were established in the present work and the observed agreement between experimental and calculated level energies is satisfactory (see Fig. 8) as the average difference between data and calculations is only 29 keV. The lowest spin 1^+, 2^+, and 3^+ levels are calculated to be located at 1688, 1865, and 1942 keV, respectively. They remain unobserved in the present work, as well as in all previous studies. The calculated second 10^+ level is associated with a rather pure $\nu(i_{11/2})^2$ configuration and the computed 2915-keV excitation energy matches well the observed, 2860-keV one for the level tentatively assigned as 10^+.

The strongly populated yrast 11^- state at 2508 keV has its theoretical counterpart at 2667 keV. It is calculated to be predominantly associated with the $\nu g_{9/2} j_{15/2}$ configuration (99% wave-function amplitude). Here, the spin value is lower than the $12\hbar$ maximum spin available for this coupling, herewith enabling the full involvement of the $g_{9/2} \times 3^-$ amplitude known to contribute to the $j_{15/2}$ single-particle state in ^{209}Pb [11]. Therefore, this 11^- state involves the $\nu(g_{9/2})^2 \times 3^-$ configuration and this should be reflected in the observed collectivity of this level. This is indeed the case: the reduced transition probability for the main, 1234-keV, $E3$ decay branch, extracted from the measured half-life, corresponds to a value of $B(E3) = 5.4(5) \times 10^4\,e^2\,\mathrm{fm}^6$, i.e., to a 21(2) W.u. enhanced $E3$ transition. The reduced transition probabilities were also obtained for the two other, much weaker, decay branches from the 11^- level. The 706-keV transition, with the $B(E1) = 6(1) \times 10^{-9}$ W.u. strength, is a retarded $E1$ transition and the 393-keV $M2$ branch, with the measured value of $B(M2) = 0.27(6)$ W.u., fits well within the systematics of $B(M2)$ values determined for the $j_{15/2} \rightarrow i_{11/2}$ transitions observed in ^{209}Pb [11] and ^{208}Pb [2]. The second 11^- level,

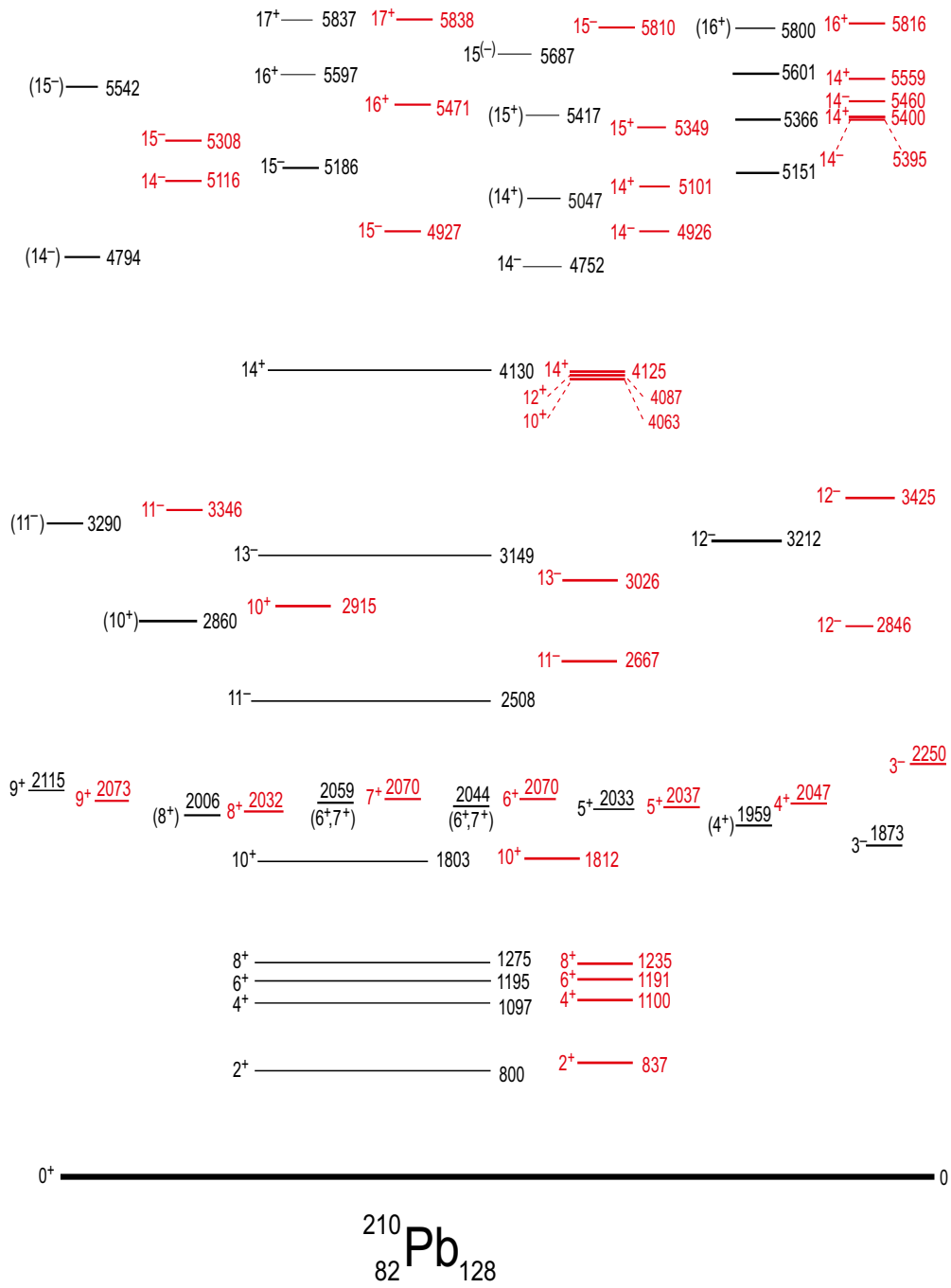

FIG. 8. Comparison between experimental and calculated states in ^{210}Pb. For transparency, a format similar to that adopted for the level scheme of Fig. 3 was used with the calculated levels (red online) placed to the right of the experimental counterparts (black) (see text). All levels are labelled with the experimental and calculated level energies, respectively.

calculated to be located at 3346 keV and associated with a 98.8% pure $\nu i_{11/2} j_{15/2}$ configuration, is close to the experimental level at 3290 keV and supports the adopted tentative I^{π} assignment.

Good agreement of the calculated 13^-, 3026-keV excitation energy with the strongly populated and unambiguously assigned 13^-, 3149-keV yrast level clearly supports the calculated pure (100%) $\nu i_{11/2} j_{15/2}$ structure of this state. As was the case with the first 11^- level discussed above, here as well octupole collectivity should be expected to contribute to the structure of this state and the 1346-keV $E3$ decay branch to the $\nu i_{11/2} g_{9/2}$, 10^+ level should be enhanced. The upper half-life limit of 2.3 ns established for the 13^- level (see above) combined with the observed decay branching leads to a lower limit for the enhancement of this 1346-keV $E3$ transition of $B(E3) > 10$ W.u. On the other hand, the situation is less clear for the experimental 12^- level at 3212 keV for which two calculated counterparts can be con-

sidered. The first 12^- state, with a practically pure $\nu g_{9/2} j_{15/2}$ structure, is computed to be located at a much lower energy of 2846 keV, while the second is predicted to be at 3425 keV and to correspond to a pure $\nu i_{11/2} j_{15/2}$ configuration. Whereas the search for the second experimental 12^- level was unsuccessful, the observed sizable population of the 3212-keV level clearly emphasizes its yrast character. For such a state, the calculated, much lower $\nu g_{9/2} j_{15/2}$ structure is then the more likely assignment. The higher measured excitation energy may be due to the fact that the assigned $\nu g_{9/2} j_{15/2}$ configuration effectively blocks the $g_{9/2} \times 3^-$ amplitude usually present when the $j_{15/2}$ neutron is invoked and this may not have been taken fully into account in the $j_{15/2}$ single-particle energy used in the calculations. The highest spin parity available for the simple two-neutron structure is $I^\pi = 14^+$ and corresponds to the state observed at 4130 keV and calculated at nearly the same energy. It is associated with a pure $\nu(j_{15/2})^2$ configuration. In Fig. 8, the nature of this level is emphasized by also showing the calculated 12^+ and 10^+ levels of the same configuration, although the latter were not observed in the present investigation. It is remarkable that the 1622-keV $E3$ branch was observed in competition with the 981-keV $E1$ one in the depopulation of this level. However, the determination of transition rates would require a dedicated experiment focusing on the measurement of short half-lives in ^{210}Pb.

All other states established in the present study involve $1p$-$1h$ excitations of the ^{208}Pb core. They are correlated in Fig. 8 with the calculated levels in a more arbitrary way, thereby reflecting the complexity of the observed level structure. Here, the wave functions of most of the computed states are complex and the dominance of any particular configuration becomes rare. Nevertheless, examples of the latter situation are the two lowest 15^- levels where, in both cases, the $\nu g_{9/2} i_{11/2}$ 10^+ structure is coupled to the lowest 5^- ^{208}Pb core excitation. In the calculated 4927-keV yrast level, this core excitation contributes to the wave function predominantly through the $\pi(s_{1/2})^{-1} h_{9/2}$ configuration of 84% amplitude, and the second 15^- level, predicted at 5308 keV, involves the $\pi(d_{3/2})^{-1} h_{9/2}$ structure with an 81% amplitude. To illustrate the more frequently observed complexity of state configurations, one may consider the lowest 16^+ level calculated at 5471 keV and correlated with the 5597-keV experimental yrast 16^+ state. The calculated wave function of this state involves 17 configurations with amplitudes larger than 1%, the largest of which, with a 22% value, is associated with the $\nu i_{11/2} j_{15/2} \times \pi(d_{3/2})^{-1} h_{9/2}$ structure. In the latter, the proton $1p$-$1h$ excitation represents an important part of the 3^- octupole excitation in ^{208}Pb and the observed $E3$ 2448-keV decay branch to the 13^- $\nu i_{11/2} j_{15/2}$ level supports the calculated configuration. In addition, it should be noted that the energy of this $E3$ transition is close to that of the 2419-keV $E3$ transition observed above the $\nu j_{15/2}$ state in ^{209}Pb [20], herewith indicating that the $i_{11/2}$ neutron in ^{210}Pb remains an inactive spectator in this 3^- coupling.

In Fig. 8, the calculated levels were sorted and placed to the right of experimental states based on the closeness of the respective energies. Although, in some cases, this ordering and correspondence may not be entirely certain, in general the agreement between calculated and experimental level energies is rather satisfactory. Most importantly, the calculations confirm the experimental observation that, in the region above 4.5 MeV, the depopulation of high-spin levels is strongly fragmented. No sequence of states stands out that could pick up the γ-ray flux typical for the yrast decay. Further calculations extending to 8.4 MeV in excitation energy and $I = 20\hbar$ in spin suggest that this situation also persists in this range.

V. EVIDENCE FOR A NEW β-DECAYING HIGH-SPIN ISOMER IN ^{210}Tl

During the search for the possible presence of other long-lived states above the 8^+ isomer in ^{210}Pb, the inspection of delayed γ-ray spectra provided an interesting, but puzzling, observation: of all the γ rays identified above this long-lived state, only the 528.1-keV transition depopulating the 10^+, 1802.9-keV level exhibited a relatively intense delayed component. The association of this delayed 528.1-keV γ ray with any other nucleus was excluded, based on the available coincidence relationships, and the observed line was firmly identified as the ^{210}Pb $10^+ \rightarrow 8^+$ transition. Whereas the analysis of Sec. III above established that the 10^+ level half-life had to be shorter than 3 ns, it had to be concluded that there was population of this state from another unknown isomer. The presence of any such long-lived state with an energy close to the 10^+ level in ^{210}Pb appeared to be unlikely and difficult to reconcile with the available shell-model calculations. Therefore, a more natural explanation was considered: the existence of a new high-spin isomer in ^{210}Tl that would populate the 10^+ level through its β-decay branch to the ^{210}Pb daughter. The flat time distribution observed for the delayed component of the 528.1-keV transition sets a lower limit of 3 μs for the half-life, a value compatible with expectations for a β-decay process. The analysis also indicated that, of all the $\nu g_{9/2} i_{11/2}$ levels established in ^{210}Pb, only the 10^+ state was populated by this β-decay branch and, in particular, no indication was found for the presence of the 9^+ state in the delayed spectra. This would suggest a possible $I^\pi = 11^+$ or higher spin assignment for the postulated β-decaying ^{210}Tl isomer.

As a next step, shell-model calculations of the ^{210}Tl levels were carried out to check that such an isomeric state could be present in this nucleus. The results of these calculations can be found in Fig. 9. The calculated $I^\pi = 5^+$ ground state fits well with the tentative spin-parity assignment proposed in the study of Ref. [5] for the ^{210}Tl β decay [$T_{1/2} = 1.30(3)$ min]. Practically all of the calculated higher-lying levels, up to a 1.2-MeV excitation energy, are of positive parity and arise predominantly from the $\pi(s_{1/2})^{-1} \nu(g_{9/2})^3$ configuration where various spin couplings are possible up to the $I = 11$ maximum value. The 11^+ level is calculated to be located at 1127 keV (Fig. 9) and the sequence of other computed levels lying close in energy is such that the possibility of a 11^+ long-lived isomer should not be discounted. With the 10^+ level calculated nearly 200 keV higher in energy, only the 9^+ level, computed to be 100 keV lower, would possibly destroy the isomerism by providing a $11^+ \rightarrow 9^+$ fast decay path. However, a relative 100-keV shift reversing the energies of the 11^+ and 9^+ levels is certainly within the

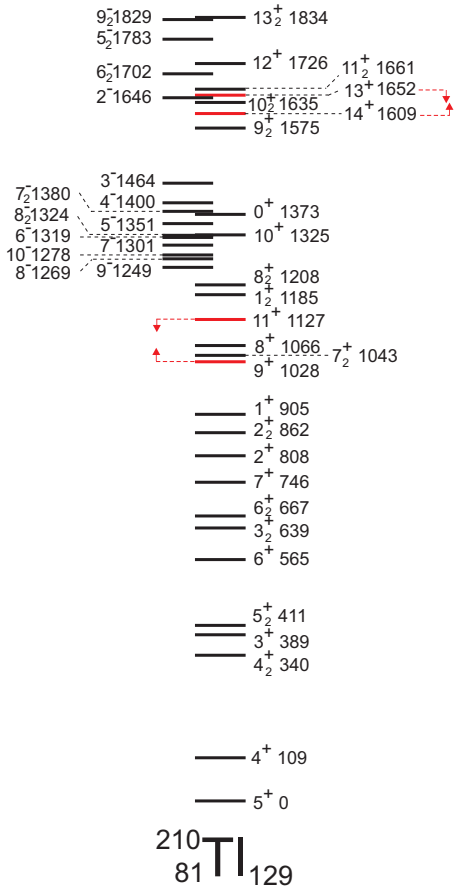

FIG. 9. Calculated shell-model levels in the three-neutron one proton-hole ^{210}Tl isotope suggesting that, apart from the known 5^+ ground-state β decay, the 11^+ level might become a β-decaying isomer as well, as observed in the present data. This requires only a 100-keV shift that would reverse the respective positions of the 9^+ and 11^+ states. It should be noted that the calculated 14^+ level is also a candidate for an isomer, but a 43-keV lowering of the 13^+ level energy would be sufficient to destroy isomerism (see discussion in the text).

errors of the calculations so that shell-model predictions make the experimental observation of the 11^+ β-decaying isomer plausible. Nevertheless, when considering this possibility, it has to be acknowledged that this tentative 11^+ assignment to the isomer results in difficulties in the interpretation of the observed β decay, as the configurations of the initial and final states would be significantly different. Clearly, more detailed information is required to resolve this issue. Surprisingly, the 14^+ level calculated at 1609 keV (Fig. 9), with a predominant $\pi(s_{1/2})^{-1}\nu i_{11/2}(g_{9/2})^2$ configuration, is another candidate for a similar long-lived state. In this case, the situation is opposite as the 13^+ level is calculated to be located only 43 keV above the 14^+ state and it would need to be somewhat lower in actuality to provide a deexcitation path avoiding the presence of such a higher-spin isomer for which there is no evidence in the data.

To support further the proposed existence of the β-decaying isomer in ^{210}Tl, a dedicated analysis was carried out

TABLE III. Ratio of the observed production yields of the anticipated 11^+ β-decaying isomer in ^{210}Tl and of the 8^+ isomer in ^{210}Pb in reactions used in the present study and listed in the first column. See text for a detailed discussion.

Colliding system	^{210}Tl$(11^+)/^{210}$Pb$(8^+) \times 10^3$
^{208}Pb + ^{64}Ni	0 (10)
^{208}Pb + ^{76}Ge	4 (1)
^{208}Pb + ^{82}Se	6 (3)
^{208}Pb + ^{208}Pb	6.7 (5)
^{238}U + ^{208}Pb	80 (40)
^{238}U + ^{48}Ca	120 (30)

to determine its population in the various reactions used in the present investigation. In each case, the counts in the 98- and 528-keV γ rays were integrated in the delayed spectra obtained with double coincidence gates placed on the 297- and 800-keV ^{210}Pb transitions in *ddd* cubes sorted with a full 800-ns range for the delayed-time parameter. The ratios of the intensities of the 528- and 98-keV transitions, corrected for efficiency and electron conversion, then represent—at least approximately—the relative production yields of the anticipated ^{210}Tl isomer and of the strongly populated ^{210}Pb 8^+ one. Yield ratios measured in this way are listed in order of increasing population of the ^{210}Tl isomer in Table III for six reactions. Whereas one may notice a small increase in the relative population of the anticipated ^{210}Tl long-lived state with the mass number of the various projectiles bombarding the ^{208}Pb targets, a more striking rise is observed for reactions with ^{238}U targets. In particular, complex multinucleon transfer reactions occurring in the ^{48}Ca + ^{238}U collisions are found to populate effectively the neutron-rich part of the ^{208}Pb region, but do not produce ^{210}Pb with large cross sections. Hence, the largest value of the relative yields in Table III supports production via multinucleon transfer, and the overall picture obtained in this way fits well with the presence of a new β-decaying isomer in ^{210}Tl. While this conclusion appears to be rather certain, based on the present observations, a full identification is desirable. This will require a new, dedicated experiment with the goals of determining the half-life and of firmly establishing the spin and parity quantum numbers of the isomer.

In the same analysis, the presence of the known (5^+) ^{210}Tl ground-state β decay could be established as well although, in this case, a quantitative estimate of the production yield was impossible. This decay has been studied with scintillator detectors in 1964 [4,5], using the weak ^{210}Tl fraction populated in the rare α decay of ^{214}Bi accumulated from the ^{226}Ra decay chain. Apart from the intense 297- and 800-keV γ rays, known to belong to the ^{210}Pb $4^+ \rightarrow 2^+ \rightarrow 0^+$ sequence, the list of transitions reported in the ^{210}Tl (5^+) ground-state decay [4,5] includes two strong ($I_\gamma \sim 20\%$) lines with respective 1210(20)- and 1310(20)-keV energies, both of which are located above the 4^+ level. Since the strong population of the 8^+ isomer in ^{210}Pb excluded the use of the 297- and 800-keV lines from the search, the delayed spectra coincident with the double 297–800-keV gate were inspected for these

two other transitions. In most of the data obtained for the reactions listed in Table III, such spectra revealed the presence of weak 1220(1)- and 1319(1)-keV γ lines; these are most likely the transitions established in the earlier study [4,5], but observed here with more precise energies. Summarizing, one may conclude that β decays have been observed in the present study from both the 5^+ ground state and a new isomer, tentatively assigned as 11^+.

VI. CONCLUSIONS

The level structure of ^{210}Pb has been studied in γ-γ coincidence measurements following deep-inelastic reactions involving mostly the ^{208}Pb + ^{208}Pb system. Additional support was provided by experiments using several other DIHIR. The level scheme, delineated up to an excitation energy of nearly 6 MeV and a spin I of $17\hbar$, validated the level scheme proposed earlier while adding also a number of previously unobserved states. As a result of the large spin alignments achieved in the ^{210}Pb reaction product, the angular-distribution analysis enabled firm spin-parity assignments to most of the strongly populated states while also facilitating tentative, but likely, assignments to other, weakly populated levels.

Accurate excitation energies of the 8^+ and 6^+ yrast states were determined based on the firm identification of the low-energy $E2$ transitions involved in the isomeric decays. The half-life of the 6^+ level was determined to be nearly twice as long as measured previously. While earlier work had identified the 10^+ state arising from the $g_{9/2}\, i_{11/2}$ coupling of two neutrons to the highest possible spin, six other, lower-spin, levels of this multiplet have now been identified as well. The 14^+ level associated with the $\nu(j_{15/2})^2$ configuration was firmly established. Thus, the highest spin value reachable by two-neutron excitations has been reached and all the higher-lying states were interpreted as involving $1p$-$1h$ excitations of the ^{208}Pb core.

Large-scale shell-model calculations including these $1p$-$1h$ core excitations have been performed. In general, they provide a satisfactory agreement between the experimental and calculated states. Specifically, there is a clear one-to-one correspondence and a quantitative agreement between data and calculations for levels associated with two-neutron excitations involving pure configurations. For higher-spin levels, the correspondence is less evident, but there as well the agreement between experimental and calculated level energies is satisfactory. Furthermore, the calculations account for the large fragmentation of the γ-ray intensity observed in the high-spin part of the level scheme. This absence of a favorable yrast decay path gathering significant decay strength is seemingly the main obstacle to an extension of the present study of ^{210}Pb levels into an excitation-spin region beyond 6 MeV and $I = 17\hbar$.

The presence of firmly established $E3$ transitions in the depopulation of four ^{210}Pb states was discussed in terms of configurations involving the collective octupole excitation of the ^{208}Pb core. For the 11^- and 13^- yrast levels, the half-life measurements established $E3$ transition strengths of 21(2) W.u. and $>$ 10 W.u., respectively. These enhancements are of the same magnitude as that of the $j_{15/2} \rightarrow g_{9/2}\, E3$ transition rate in ^{209}Pb [11], and confirm the involvement of the $j_{15/2}$ neutron in the structure of both states. Although the rates for two other $E3$ transitions remain unknown, the $E3$ decay branch from the 14^+ $(j_{15/2})^2$ level is likely of a similar nature, and the high energy of the $E3$ transition depopulating the yrast 16^+ level is notably close to that of the octupole ^{208}Pb core excitation observed above the $j_{15/2}$ level in ^{209}Pb [20].

Finally, the population of the yrast 10^+ level observed in the decay of a hitherto unknown long-lived state indicated the existence of a new β-decaying isomer in ^{210}Tl. Shell-model calculations, together with the production yields observed with a number of reactions used in the present study, supported this finding and enabled a tentative $I^\pi = 11^+$ spin-parity assignment to this new ^{210}Tl isomer.

ACKNOWLEDGMENTS

The authors thank the ATLAS operating staff for the efficient running of the accelerator during the long series of experiments performed for the present study and J. P. Greene for target preparations. Contributions by researchers who participated in the early phases of this study, which were reported in earlier publications, are gratefully acknowledged. This work was supported by the Polish National Science Center, Projects No. 2012/07/N/ST2/02861 and No. 2016/21/B/ST2/02195, the US Department of Energy, Office of Science, Office of Nuclear Physics, under Contract No. DE-AC02-06CH11357 (ANL), and Grants No. DE-FG02-97ER41041 (UNC), No. DE-FG02-97ER41033 (TUNL), and No. DE-FG02-94ER40834 (UM), NSF Grant No. PHY-1404442, the Australian Research Council, and the Science and Technology Facilities Council (STFC), UK. This research used resources of ANL's ATLAS facility, a DOE Office of Science User Facility.

[1] A. Heusler, R. V. Jolos, T. Faestermann, R. Hertenberger, H.-F. Wirth, and P. von Brentano, Phys. Rev. C **93**, 054321 (2016).
[2] R. Broda, R. V. F. Janssens, Ł. W. Iskra, J. Wrzesiński, B. Fornal, M. P. Carpenter, C. J. Chiara, N. Cieplicka-Oryńczak, C. R. Hoffman, F. G. Kondev, W. Królas, T. Lauritsen, Zs. Podolyak, D. Seweryniak, C. M. Shand, B. Szpak, W. B. Walters, S. Zhu, and B. A. Brown, Phys. Rev. C **95**, 064308 (2017).
[3] R. Broda, J. Phys. G: Nucl. Part. Phys. **32**, R151 (2006).
[4] M. Shamsuzzoha Basunia, Nucl. Data Sheets **121**, 561 (2014).
[5] P. Weinzierl, E. Ujlaki, G. Preinreich, and G. Eder, Phys. Rev. **134**, B257 (1964).
[6] E. R. Flynn, G. J. Igo, R. A. Broglia, S. Landowne, V. Paar, and B. Nilsson, Nucl. Phys. A **195**, 97 (1972).
[7] D. J. Decman, J. A. Becker, J. B. Carlson, R. G. Lanier, L. G. Mann, G. L. Struble, K. H. Maier, W. Stöffl, and R. K. Sheline, Phys. Rev. C **28**, 1060 (1983).

[8] M. Rejmund, K. H. Maier, R. Broda, M. Lach, J. Wrzesiński, J. Agramunt, J. Blomqvist, A. Gadea, J. Gerl, M. Górska, H. Grawe, M. Kaspar, I. Kozhoukharov, I. Peter, H. Schaffner, R. Schubart, Ch. Schlegel, G. Stengel, S. Wan, and H. J. Wollersheim, Z. Phys. A **359**, 243 (1997).

[9] G. J. Lane, R. Broda, B. Fornal, A. P. Byrne, G. D. Dracoulis, J. Blomqvist, R. M. Clark, M. Cromaz, M. A. Deleplanque, R. M. Diamond, P. Fallon, R. V. F. Janssens, I. Y. Lee, A. O. Macchiavelli, K. H. Maier, M. Rejmund, F. S. Stephens, C. E. Svensson, K. Vetter, D. Ward, I. Wiedenhöver, and J. Wrzesiński, Nucl. Phys. A **682**, 71 (2001).

[10] I. Y. Lee, Nucl. Phys. A **520**, c641 (1990); R. V. F. Janssens and F. S. Stephens, Nucl. Phys. News **6**, 9 (1996).

[11] J. Chen and F. G. Kondev, Nucl. Data Sheets **126**, 373 (2015); F. G. Kondev, ENSDF update, June 14, 2015.

[12] R. Broda, K. H. Maier, B. Fornal, J. Wrzesiński, B. Szpak, M. P. Carpenter, R. V. F. Janssens, W. Królas, T. Pawłat, and S. Zhu, Phys. Rev. C **84**, 014330 (2011).

[13] N. Cieplicka, K. H. Maier, B. Fornal, B. Szpak, R. V. F. Janssens, M. Alcorta, R. Broda, M. P. Carpenter, C. J. Chiara, C. R. Hoffman, B. P. Kay, F. G. Kondev, W. Królas, T. Lauritsen, C J. Lister, E. A. McCutchan, T. Pawłat, A. M. Rogers, D. Seweryniak, N. Sharp, W. B. Walters, J. Wrzesiński, and S. Zhu, Phys. Rev. C **86**, 054322 (2012).

[14] B. A. Brown, A. Etchegoyen, W. D. M. Rae, N. S. Godwin, W. A. Richter, C. H. Zimmerman, W. E. Ormand, and J. S. Winfield, MSU-NSCL Report No. 524, 1985.

[15] B. A. Brown, Phys. Rev. Lett. **85**, 5300 (2000).

[16] E. K. Warburton and B. A. Brown, Phys. Rev. C **43**, 602 (1991).

[17] G. H. Herling and T. T. S. Kuo, Nucl. Phys. A **181**, 113 (1972).

[18] A. Hosaka, K. I. Kubo, and H. Toki, Nucl. Phys. A **444**, 76 (1985).

[19] G. Bertsch, J. Borysowicz, H. McManus, and W. G. Love, Nucl. Phys. A **284**, 399 (1977).

[20] M. Rejmund, K. H. Maier, R. Broda, B. Fornal, M. Lach, J. Wrzesiński, J. Blomqvist, A. Gadea, J. Gerl, M. Górska, H. Grawe, M. Kaspar, H. Schaffner, C. Schlegel, R. Schubart, and H. J. Wollersheim, Eur. Phys. J. A **1**, 261 (1998).